



LAWRENCE
LIVERMORE
NATIONAL
LABORATORY

SPE2 Far-field Seismic Data Quicklook

R. J. Mellors, P. Harben, S. Ford, W. R. Walter, T.
Hauk, S. Ruppert, A. Pitarka, J. P. Lewis

February 16, 2012

Disclaimer

This document was prepared as an account of work sponsored by an agency of the United States government. Neither the United States government nor Lawrence Livermore National Security, LLC, nor any of their employees makes any warranty, expressed or implied, or assumes any legal liability or responsibility for the accuracy, completeness, or usefulness of any information, apparatus, product, or process disclosed, or represents that its use would not infringe privately owned rights. Reference herein to any specific commercial product, process, or service by trade name, trademark, manufacturer, or otherwise does not necessarily constitute or imply its endorsement, recommendation, or favoring by the United States government or Lawrence Livermore National Security, LLC. The views and opinions of authors expressed herein do not necessarily state or reflect those of the United States government or Lawrence Livermore National Security, LLC, and shall not be used for advertising or product endorsement purposes.

This work performed under the auspices of the U.S. Department of Energy by Lawrence Livermore National Laboratory under Contract DE-AC52-07NA27344.

SPE2 Far-field Seismic Data Quicklook

R. J. Mellors, P. Harben, S. Ford, A. Rodgers, W. R. Walter, T. Hauk, S. Ruppert, A. Pitarka, and J. P. Lewis

14 Feb 2012

Introduction. The purpose of this report is to provide a brief overview of the far-field seismic data collected by the array of instruments (Figures 1 and 2) deployed by the Source Physics experiment for shots 1 (roughly 100 kg TNT equivalent at a depth of 60 m) and shot 2, (roughly 2000 kg TNT equivalent at a depth of 45 m). 'Far-field' is taken to refer to instruments in the zone of purely elastic response at distances of 100 m or greater. The primary focus is data from the main instrument array and hence data from other groups is not considered. Infrasound data is not addressed nor any remote sensing data.

Data processing was done at LLNL in parallel with the effort at UNR. Raw reftek data was sent via hard disk from NsTec. Reftek data was converted to SEG-Y and then to SAC format. Data files were renamed according to station and channel information. Reftek logs were reviewed. These data have been reviewed for consistency with the UNR data on the server. The primary goal was quality check and a summary is provided in Tables 1 and 2.

Timing or location. Timing and location appear good for all stations. A few channels (L1-14, L2-09) show apparent errors in timing but this is likely due to a combination of a dead channel and crosstalk from an adjacent sensor.

Orientation, polarity and gain. Polarity convention varies according to instrument type (gs11d is that upward motion appears as down on the geophone). Orientation for instruments less than 2 km away are radial and tangential. Further than 2 km away, orientation is according to compass directions. Gains are nominally 1, but some stations appear to have anomalously high amplitude signals (see Table 2).

- L3-02 CHZ appeared flipped with respect to other geophones on SPE2 but not SPE1.
- L5-28 channels (CHR, CHT) appear to have been changed between SPE1 and SPE2. By comparison with SPE1 and L5-30 (presumed correct), it appears that L5-28 CHR and CHT are reversed on SPE1.
- Episensor channel assignments may be incorrect in the UNR data. Currently, they appear to be mapped from orientation/Reftek channel as R-2, T-3, Z-1 and it should be R-2, T-1, Z-3.

Geophone CHT channels were not checked for orientation due to uncertainty at the time of the report on the installed orientation and polarity.

Quality. Long-period signals on Trilliums. L3-23 CHE and L3-23 CHE2 both have longer-period drift in the same direction but different amplitudes. Low amplitude longer period signal on the N component. L5-28 CHE shows a pronounced drift. L5-36 CHE and L5-36 CHN show long period drift that is anti-correlated.

Data summary comments. As a guide to the dataset, a series of figures showing all seismograms have been created. All figures follow appendix A. Figures 4 to 13 show SPE2 with poor data shown in red and data of uncertain quality in green. Figures 13 to 18 compare SPE1 and SPE2, with SPE1 data multiplied by a factor of 10 to approximately match amplitudes of SPE2.

Seismograms have been scaled by a scale factor dependent on (range)². This allows comparison of relative amplitudes between seismograms but also permits seismograms at different ranges to appear at similar detail. All seismograms are in counts. The scaling between seismograms of a common instrument type is identical. All data has been demeaned and detrended on a window extending from the shot time to 60 seconds. Specific seismograms with long-period drift (L3-23, L5-36, L5-28) have been shifted in an attempt to bring the first record near the zero mark.

Geophones. (Figures 4 - 7) Lines 1 through 3 provided good data return, with minor problems (dead channels L1-14, L2-09, L3-16, and possible gain problems on L2-17,18, and 19). Line L4 had one dead channel (L4-7) and possible gain problems with L4-02. L4-01 showed irregular waveforms. Line 5 showed high amplitudes for stations L5-01 and L5-02, and amplitude problems on L5-05 and L5-12. It is unclear whether the high amplitudes on L5-01, L5-02, and L4-02 are due to gain problems or instrumental or site response.

Some channels show anomalously low amplitude signals with anomalous timing. It is possible that this may be a dead sensor combined with crosstalk from a nearby cable. Although speculative, this explanation matches the timing and appearance (apparent derivative) of the data (Figure 3).

After SPE1, questions were raised about the geophone (gs11d) response. As GS11D are capable of variable settings depending on the exact value of the damping and coil resistance, further effort (aided greatly by Rob Abbott of SNL) showed that the GS11D possessed 250 Ohm resistors with damping set at 50%. From the parameters (e.g. Table 3) provided for each geophone, the appropriate poles and zeros can be calculated. See Appendix A for details.

Table 3. Geophone parameters

	Res	Freq	Damp	Sens	pole-real	pole-imag	constant (v/m/s)	pole-real
Min	332.4	3.78	0.399	0.671	-9.4764E+00	-2.1778E+01	26.41732283	-9.4764E+00
Norm	349.9	4.5	0.499	0.746	-1.4109E+01	-2.4503E+01	29.37007874	-1.4109E+01
Max	367.4	5.22	0.599	0.82	-1.9646E+01	-2.6263E+01	32.28346457	-1.9646E+01

Broadbands. (Figures 8-10) Data collected on lines 3,4 and 5 was good quality except for apparent gain problems on line 3 and long period (> 10 seconds) signals on the horizontal channels on L5-36 and L5-28.

Rotational sensors. (Figure 11) Data appeared good except for a striking variation in amplitudes between line 1 and lines 2 and 10.

Accelerometers (Figure 12). The Episensor on line 2 appeared to be non-functional.

Table 1. Channels with severe problems (dead or very low amplitude/crosstalk)

Line 1:

L1-14 [possible crosstalk signal from L1-13, timing and amplitude]

Line 2:

L2-09 [bad, possible crosstalk signal from L2-10, timing and amplitude]

L2-10.CNZ, L2-10.CNR, L2-10.CNT, L2-10.DJR, L2-10.DJT [bad]

L2-13 possible crosstalk from L2-14? [timing and amplitude]

Line 3:

L3-20.DHR L3-28.CHZ [bad]

Line 4:

L4-07 [possible crosstalk from L4-05, timing and amplitude]

Line 5:

L5-05 [possible crosstalk from L5-06, timing and amplitude]

L5-12 CLZ [bad]

Table 2. Apparent gain problems

Line 1: None

Line 2:

L2-13 low ? completely bad???

L2-14 low

L2-19 high

L2-18 high

L2-17	high
Line 3:	
L3-16	low
L3-28	amplitudes not consistent between two sensors (CHR, CHT >> other
L3-28)	
Line 4:	none
Line 5:	
L5-01	high
L5-02	high
L5-03	high

Comparison between SPE1 and SPE2. As a quick comparison between SPE1 and SPE2, the two datasets were plotted on the same time scale but with SPE1 data multiplied by a factor of 10 (chosen only to roughly match amplitudes). Line 1 looked similar (Figure 13). Line 2 showed amplitude differences on L2-02 and L2-19. Line 3 appeared similar except for slightly higher frequency content. Line 4 shows amplitude differences on L4-02. For line 5, the scaling did not work well and the relative scaling for stations 7-12 appeared higher. Amplitudes for stations 1 and 2 appeared different as well.

Conclusions and Recommendations.

- Identify cause of amplitude anomalies
- Identify any switched channels between SPE1 and SPE2 (two stations were reported with changed cables by field personnel?)
- Verify possible crosstalk between sensors
- Evaluate suggested orientation/polarity of Episensors/rotational sensors.
- Develop clear plan for data collection (e.g. continuous, etc) and forward to relevant investigators prior to collection. This allows planning of analysis.

Appendix A.

Mechanical seismometer response is

$$T(\omega) = \frac{-(i\omega)^2}{\omega_0^2 + 2i\omega\omega_0 h + (i\omega)^2}, \quad (1)$$

where $\omega_0 = 2\pi f_0$ and $f_0 = T_0^{-1}$ where T_0 is the seismometer free period, and h is the damping (or fraction of critical damping).

Another way to describe the response given in eqn (1) is the pole-zero representation

$$T(\omega) = \frac{-(i\omega - z_1)(i\omega - z_2)}{(i\omega - p_1)(i\omega - p_2)}, \quad (2)$$

where z_i are the zeros and p_i are poles of the transfer function. When the mechanical seismometer response given in eqn (2) is combined with an electromagnetic transducer we have a geophone and another zero is introduced where $z_i = 0$. So, the combined response is

$$T(\omega) = c \frac{(i\omega - 0)(i\omega - 0)(i\omega - 0)}{(i\omega - p_1)(i\omega - p_2)}, \quad (3)$$

where p_1 and p_2 are the (complex) poles, there are three zeros, and c is a constant to be discussed later. Eqn (3) gives the transfer function from ground displacement to voltage. The poles are given by

$$p_1 = -\omega_0(h + \sqrt{h^2 - 1}) \quad (4)$$

$$p_2 = -\omega_0(h - \sqrt{h^2 - 1}) \quad (5)$$

So for example, a geophone with a free period of 5 s ($T_0 = 5$) and damping of 0.7 ($h = 0.7$) has three zeros and two complex poles

$$p_1 = -0.8796 - 0.8974i$$

$$p_2 = -0.8796 + 0.8974i$$

Transducer constant G is proportionality between voltage and ground motion, so for geophone G is given in V-s/m (V/m/s) and is the constant of proportionality for ground motion at $f > f_0$. To calculate the pole-zero constant c in eqn (3) G is multiplied by a standard normalization constant of 1 m·m/s.

For example, a geophone with a Sensitivity of 0.7274 V-s/inch the pole-zero constant is

$$c = 0.7274 \frac{V \cdot s}{inch} \times \frac{0.0254 inch}{m} \times 1 \frac{m}{m \cdot s} = 0.0185 \frac{V}{m}$$

The A/D converter provides another constant given in V/count and is the proportionality between the geophone and the recorder and this is a further conversion necessary to go from raw counts to displacement.

Using the Excel spreadsheet, 'Calibration Data.xls', I added three more columns: pole-real, pole-imag, and constant, where pole-real is the real pole and pole-imag is the imaginary pole, and constant is c in V/m.

One can then take each of these values and place them in a SAC pole-zero file as:

ZEROS 3

POLES 2

pole-real pole-imag

pole-real -1*pole-imag

CONSTANT constant

Conversely, one can use the 'general' option in the SAC transfer function as follows (using values from example above):

```
SAC> transfer from general nzeros 3 freeperiod 5 damping 0.7 magnification m to none
```

where m is the constant converted to the total gain at 1 Hz and is given by $m = 2\pi c$. The SAC command above returns displacement prior to A/D gain applied.

References

Havskov, J. and G. Alguacil (2002) Instrumentation in earthquake seismology.

Weilandt, E. (2009) Seismic sensors and their calibration, in New Manual of Seismological Observatory Practice (NMSOP-1), IASPEI, GFZ German Research Centre for Geosciences, Potsdam, ed. P. Bormann.

Acknowledgements. This report benefitted by the efforts of several people including Rob Abbott, Cathy Snelson-Gerlicher, Bob White, Gabe Plank, Ken Smith and Chandan Saikia.

This work performed under the auspices of the U.S. Department of Energy by Lawrence Livermore National Laboratory under Contract DE-AC52-07NA27344.

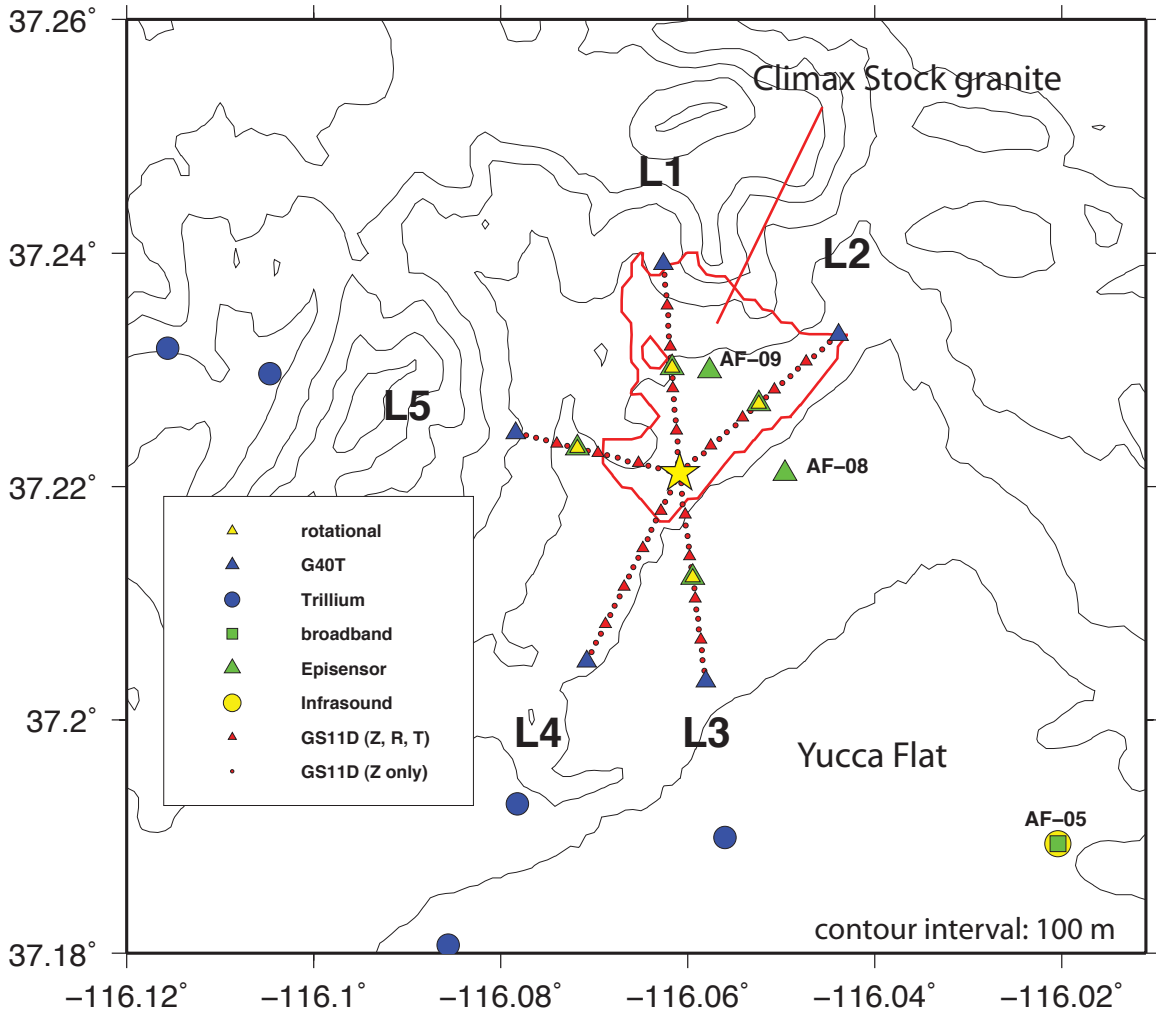


Figure 1. Map of instrument and station locations in vicinity of shot (marked by a yellow star). Station locations and instruments as denoted in the legend. Light gray lines indicate 100 m contour levels. Red line shows approximate outline of the Climax stock (granite) on surface.

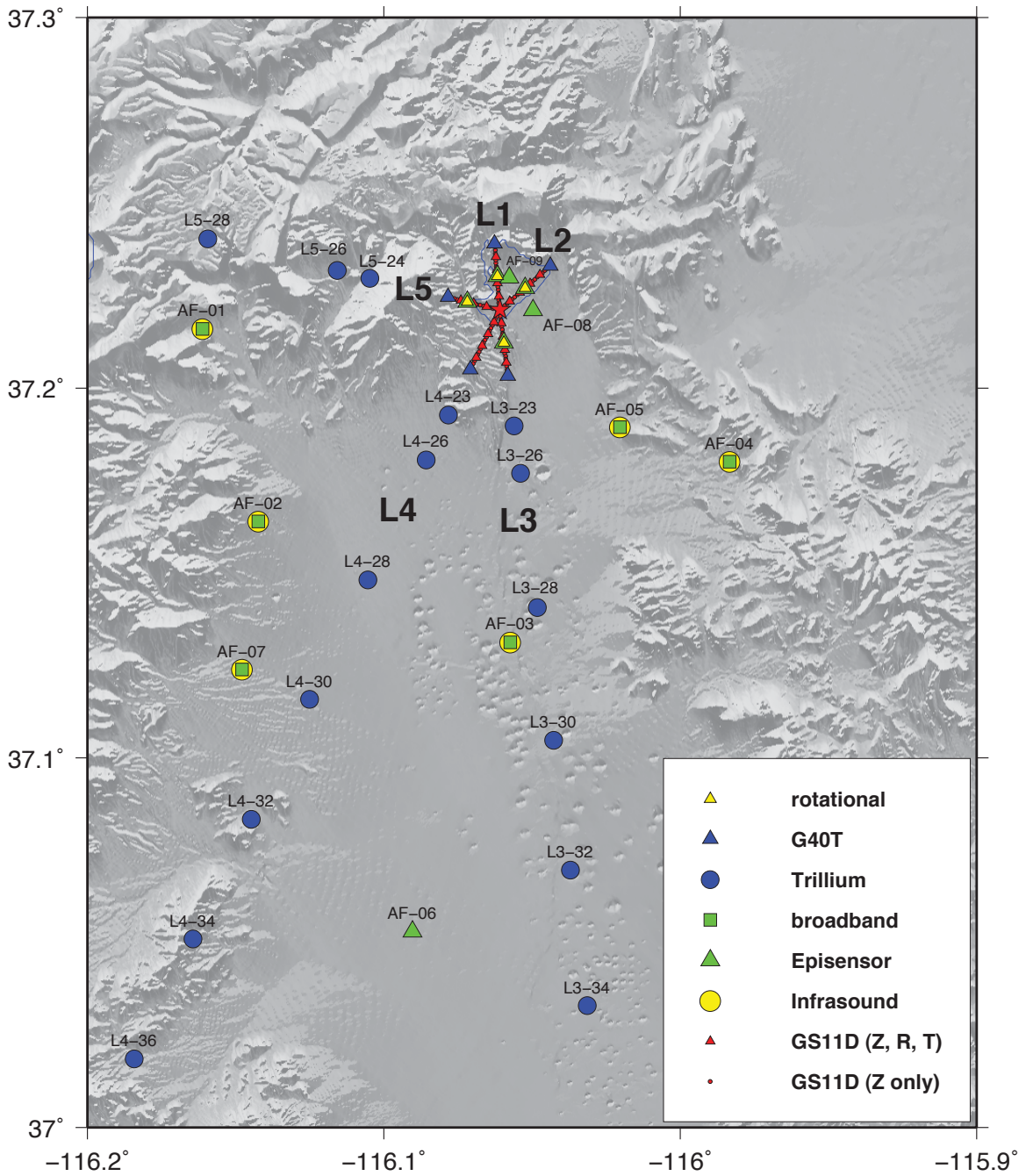


Figure 2. Map of entire deployment on shaded topography with illumination from the north. Shot point marked by star.

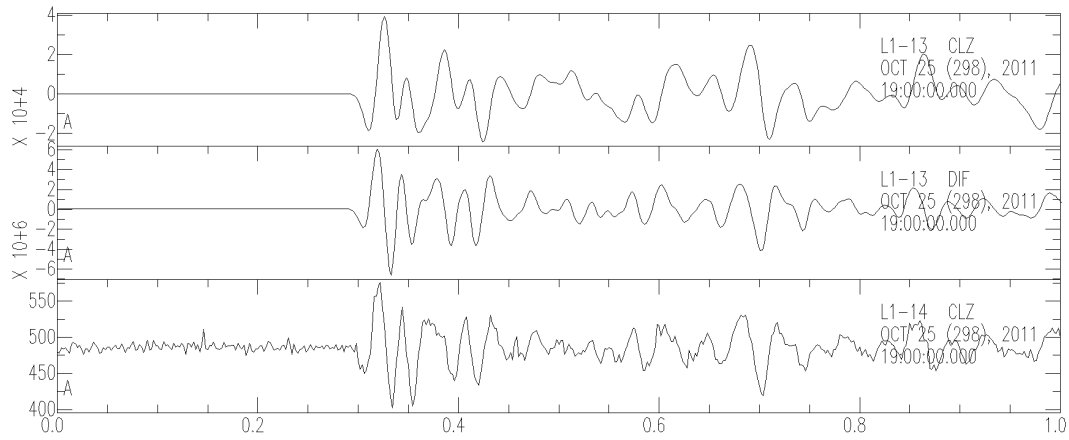


Figure 1. Example of apparent crosstalk from L1-13 to L1-14. Top trace is L1-13, middle is the derivative of L1-13 and bottom is L1-14. L1-14 may be disconnected from the sensor and picks up low amplitude crosstalk from L1-13. Note exact correspondence in time. Waveforms are not identical as crosstalk (inductive) is proportional to the change in voltage over and therefore matches the derivative of L1-13.

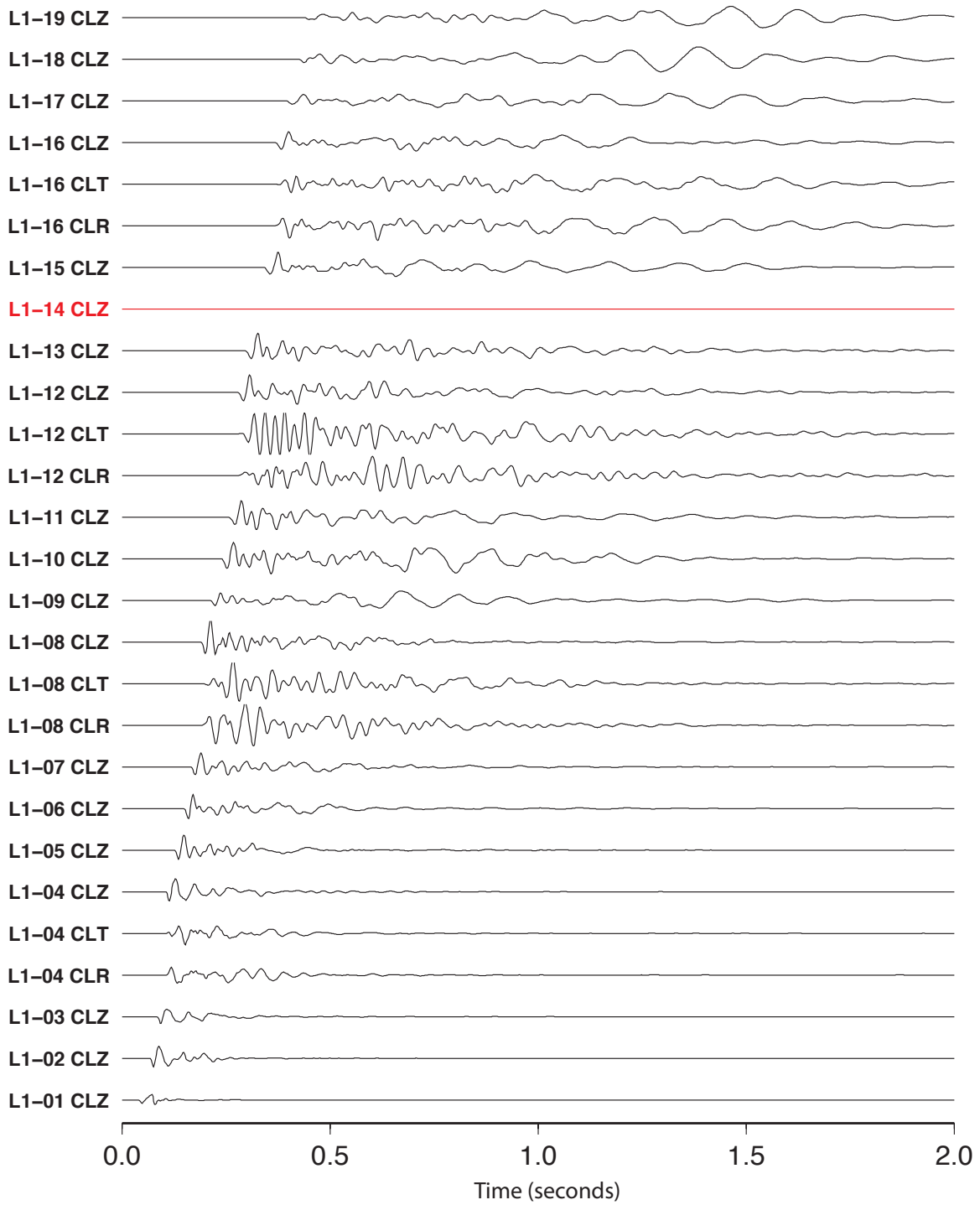


Figure 2. Geophone records from Line 1. Red indicates an instrument with problems affecting both timing and amplitude.

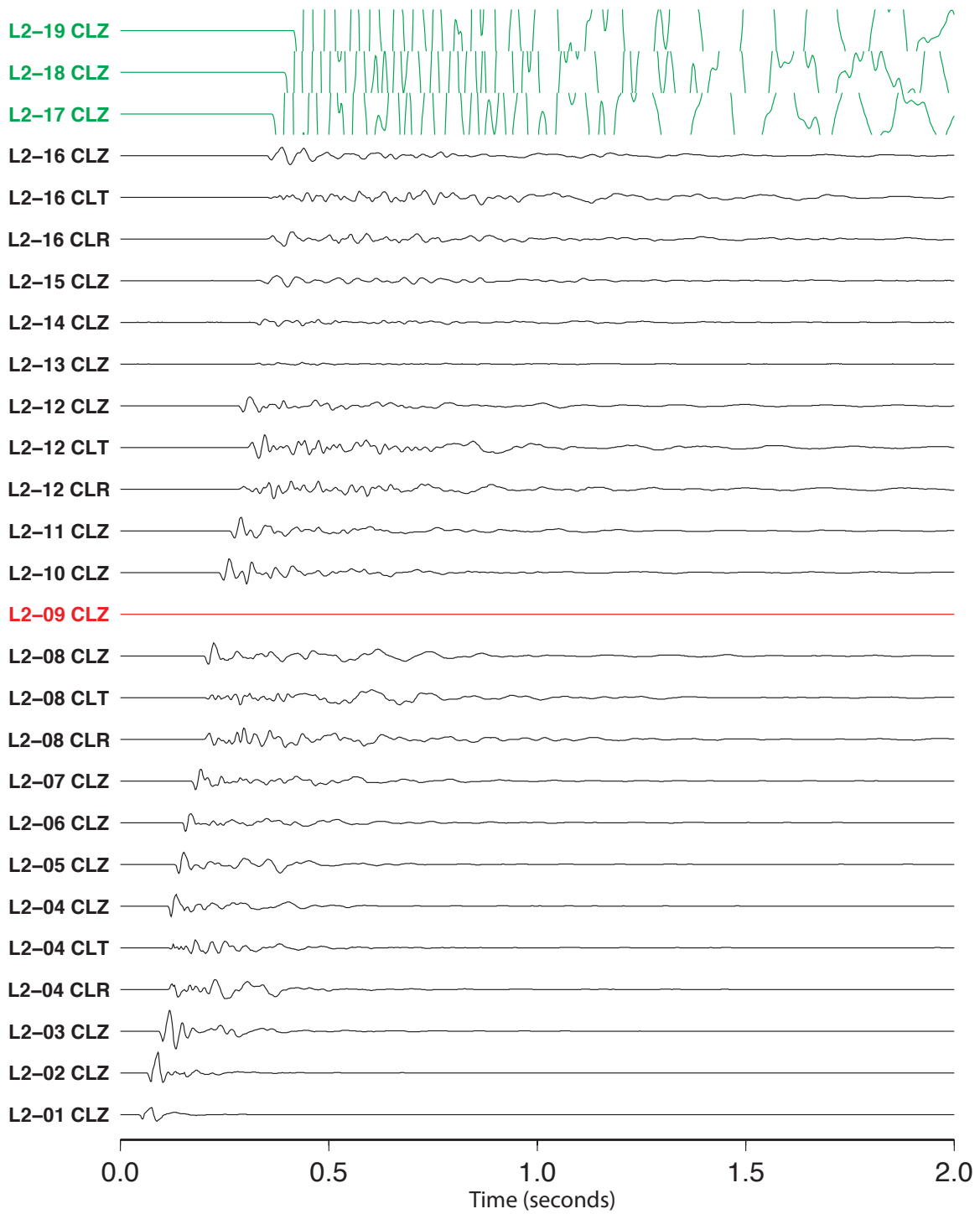


Figure 3. Geophone (gs11d) records for line 2. Numbers 17, 18, and 19 may have incorrect gain.

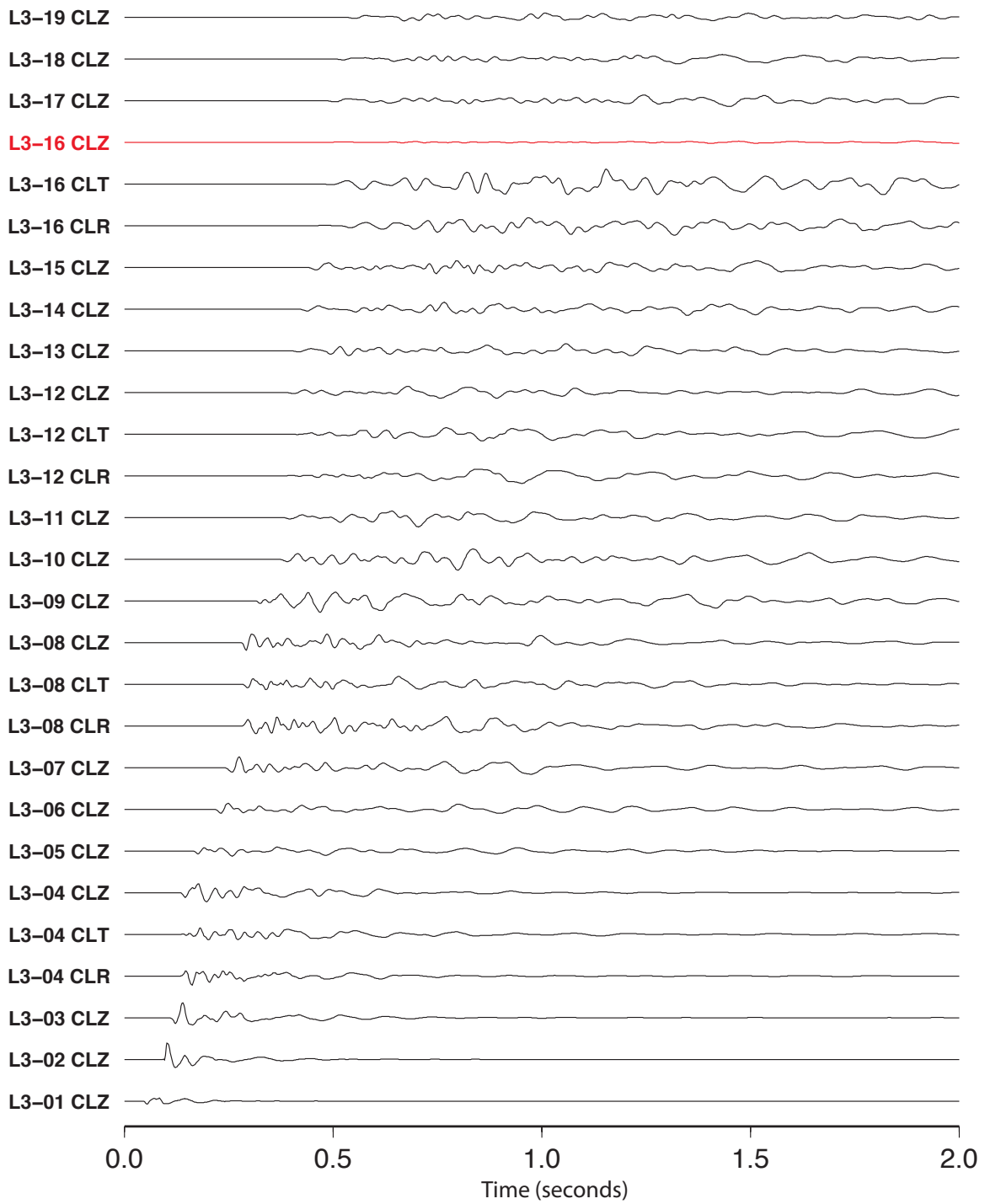


Figure 4. Geophone data for line 3.

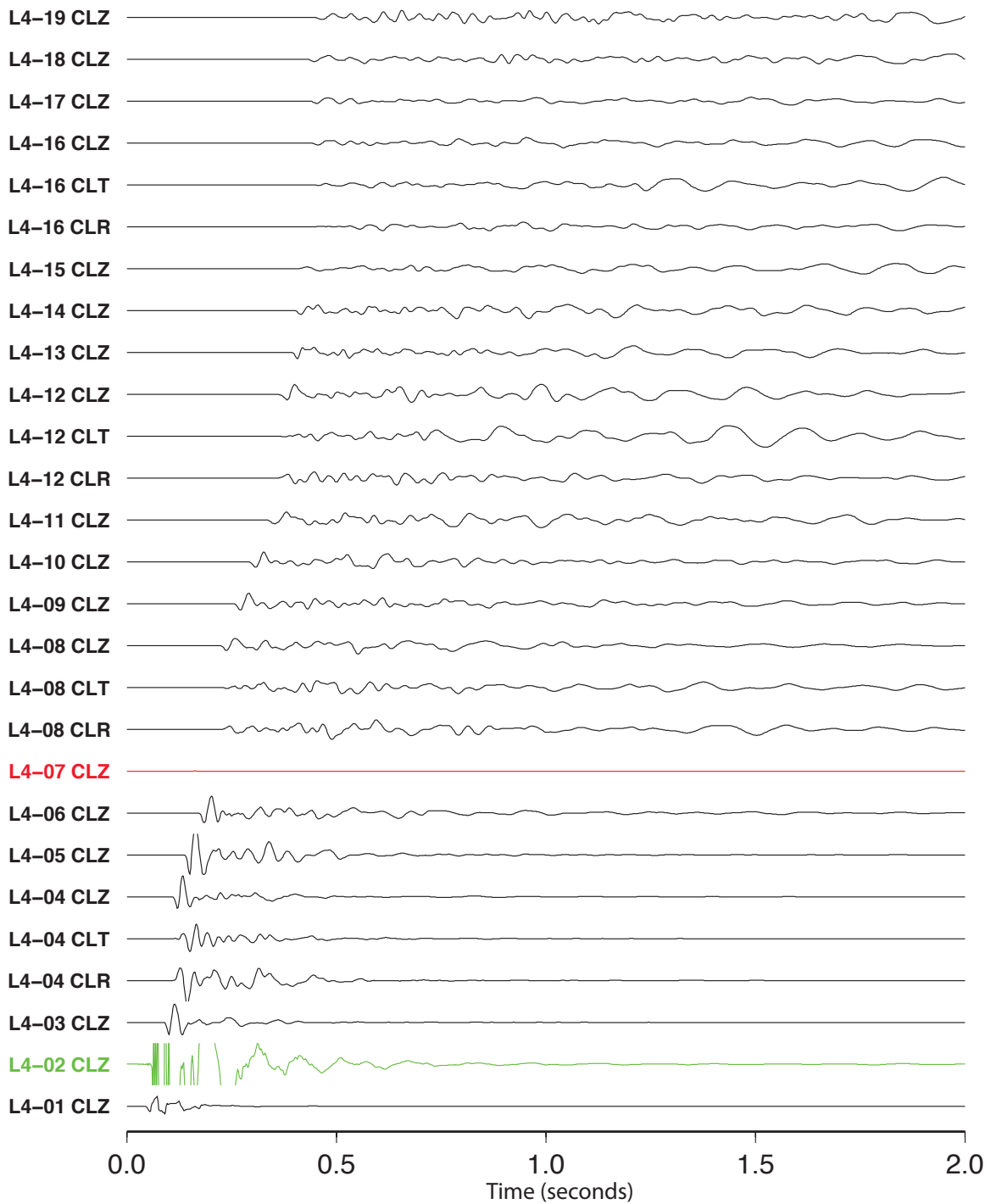


Figure 5. Geophone data for line 4. Instrument 1 may have problems; 2 may have incorrect gain. L4-07 has low amplitude and if increased, timing is apparently incorrect.

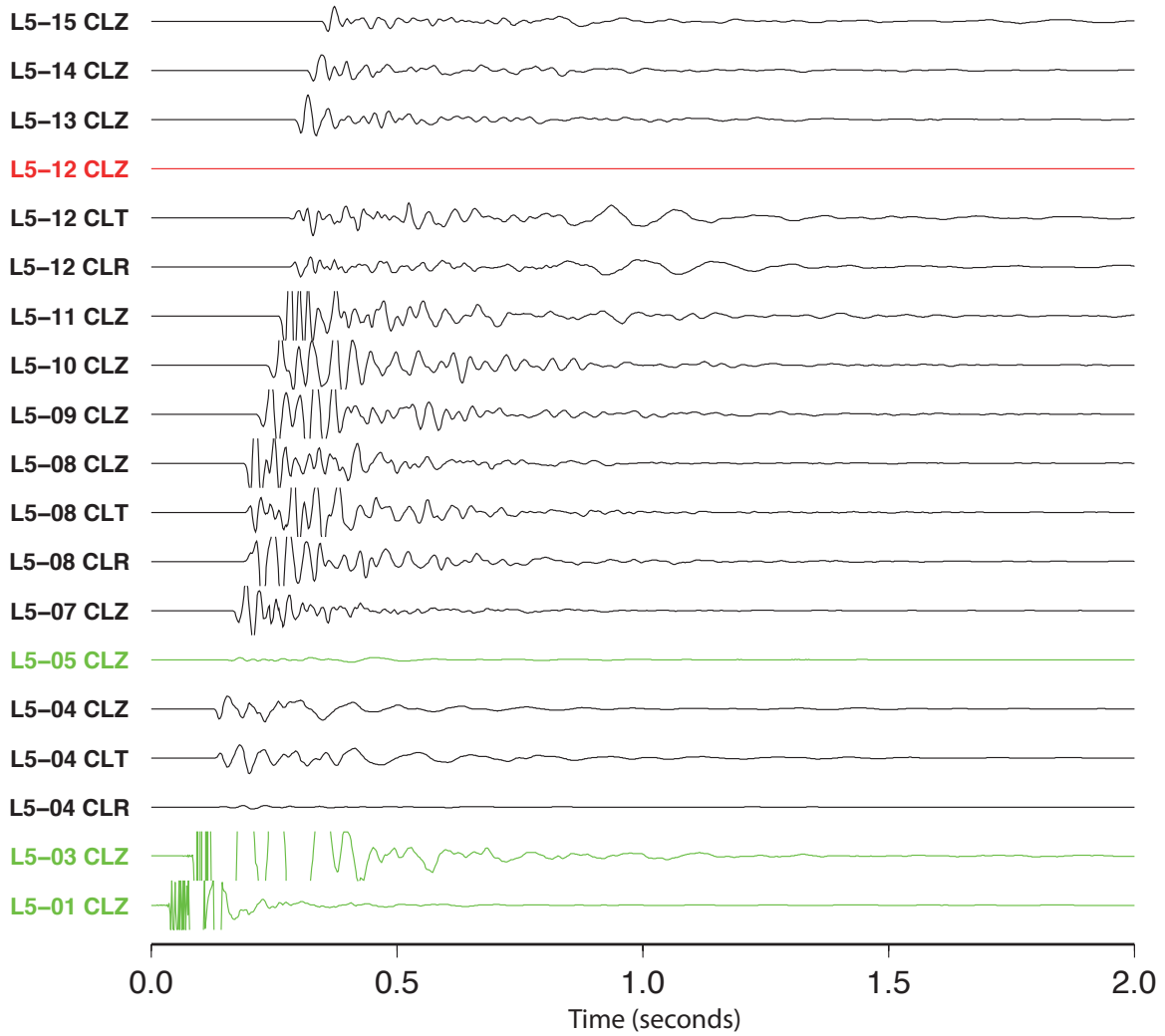


Figure 6. Geophone data for line 5. Instruments 1 and 2 show anomalous high gain; the cause is uncertain.

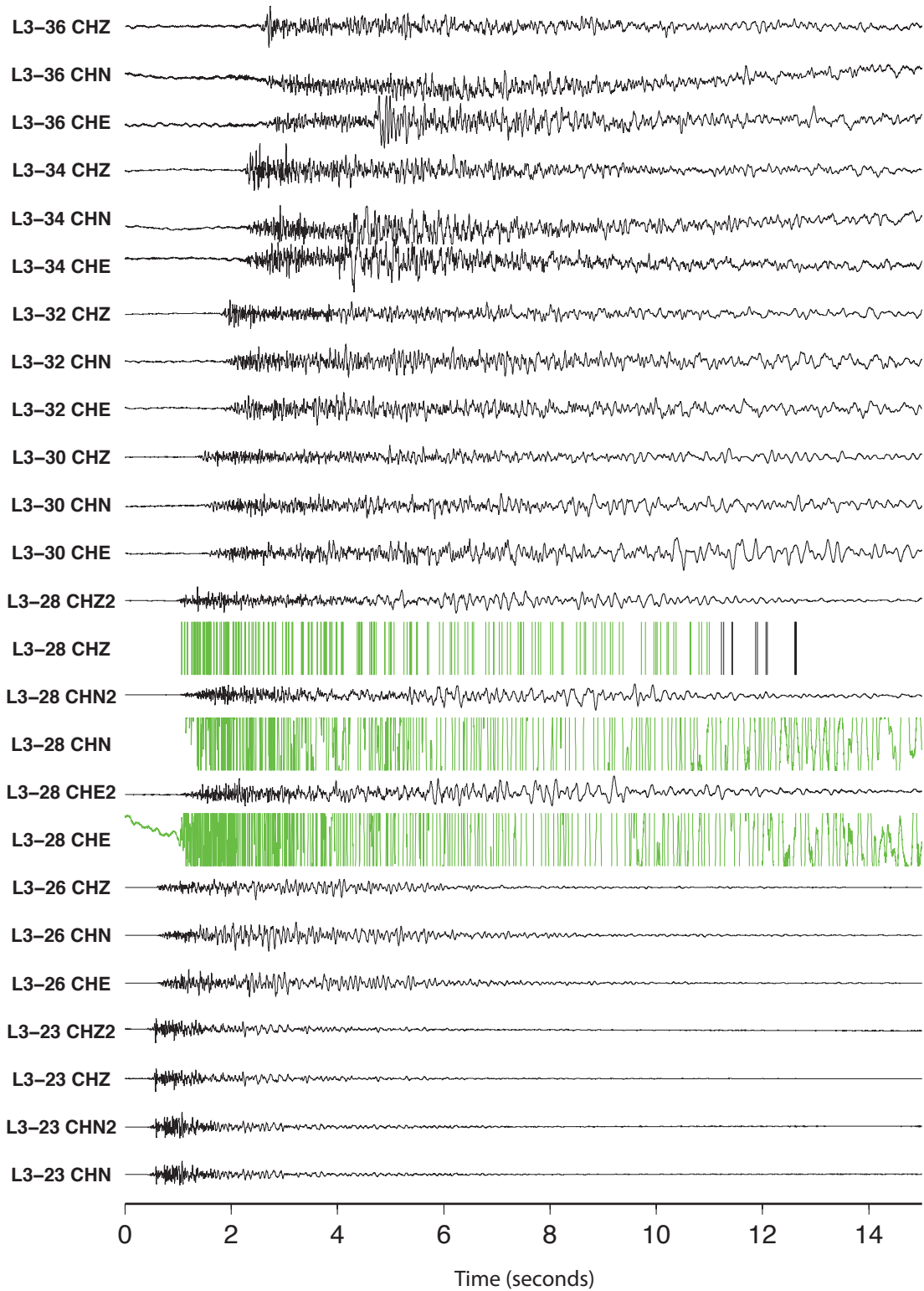


Figure 7. Data recorded by broadband instruments for line 3. Note apparent gain problems for L3-28.

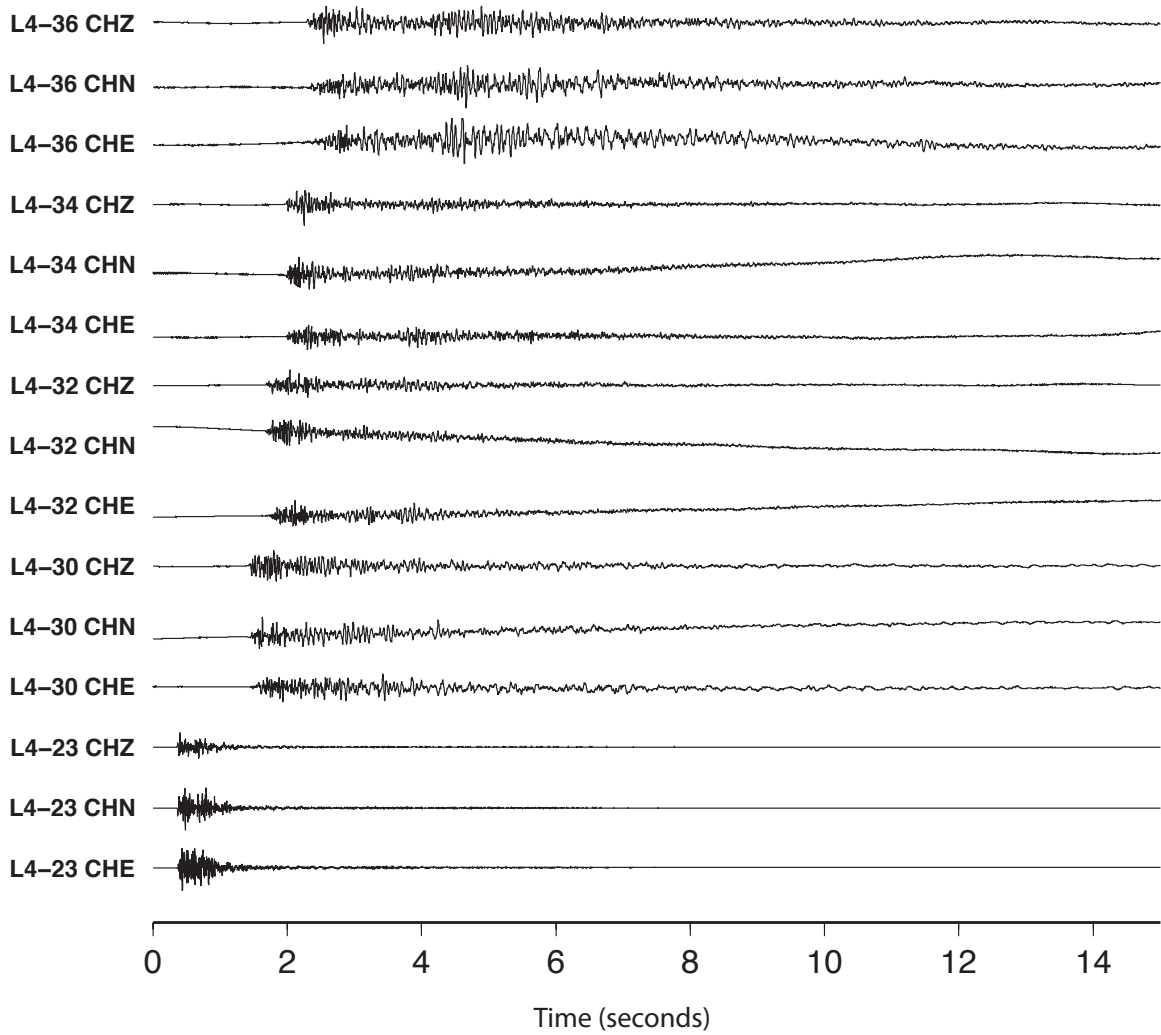


Figure 8. Broadband data for line 4.

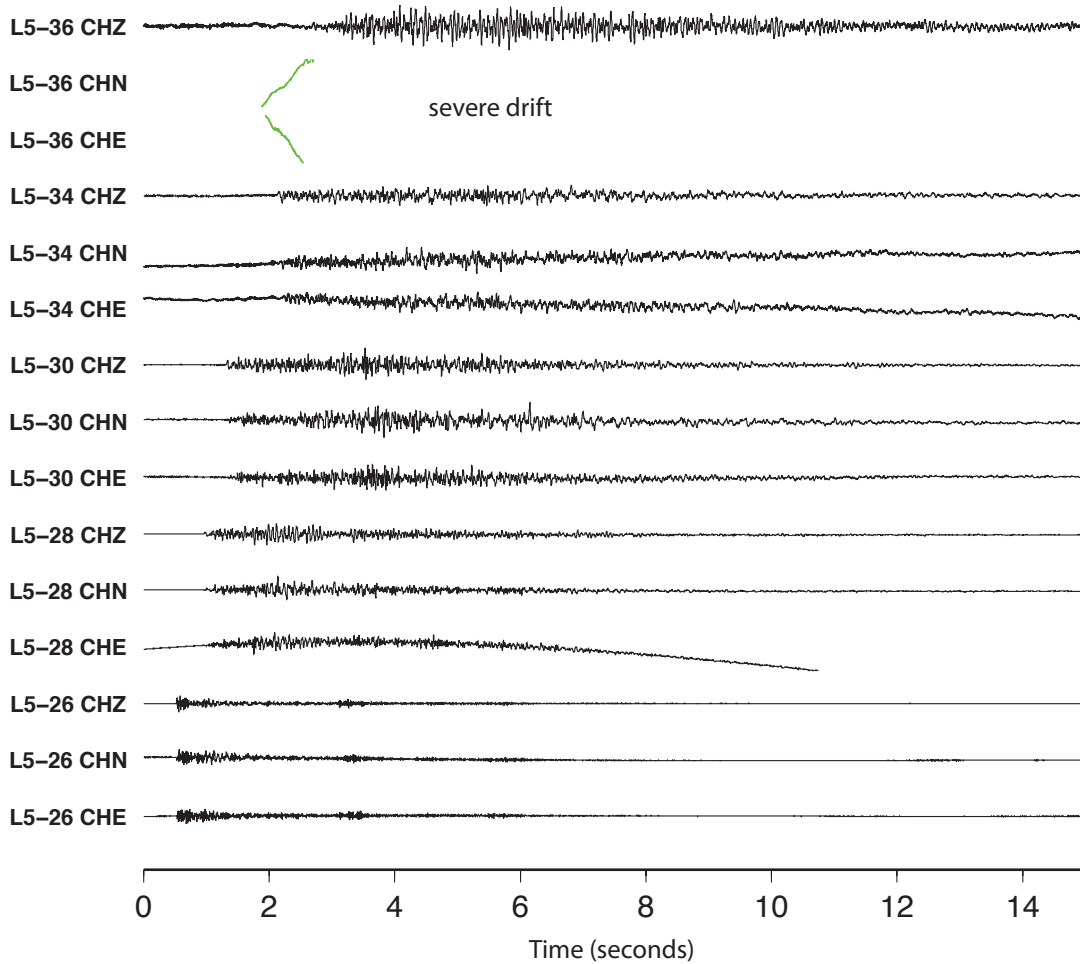


Figure 9. Broadband data for line 5. Note long period drift on some of the horizontal channels.

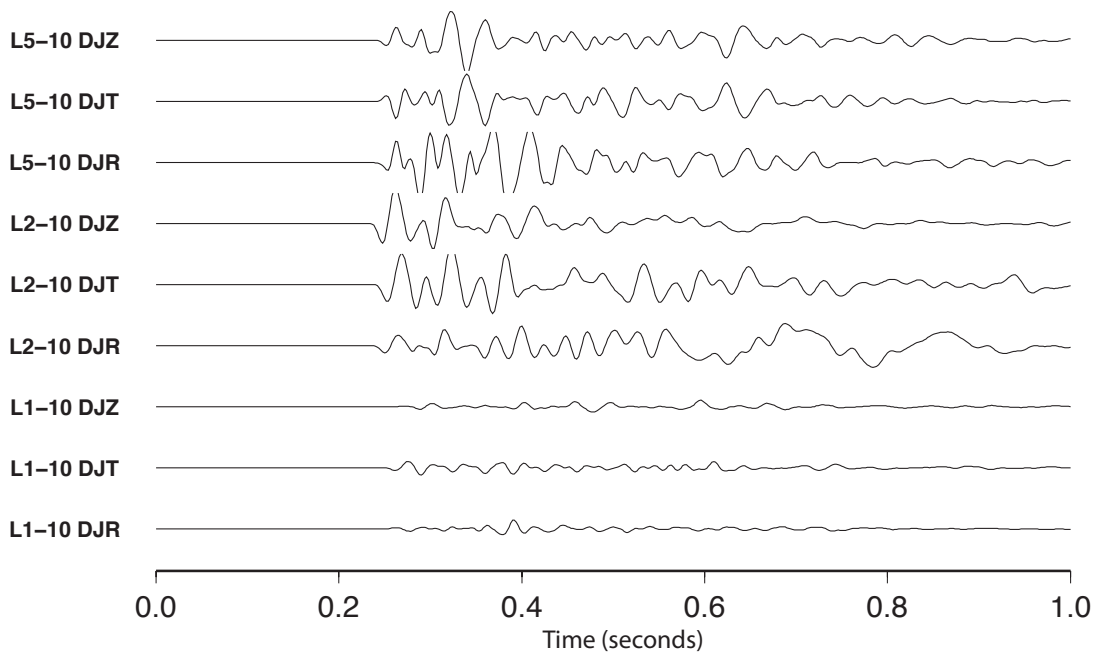


Figure 10. Rotational data for lines 1, 2 and 5.

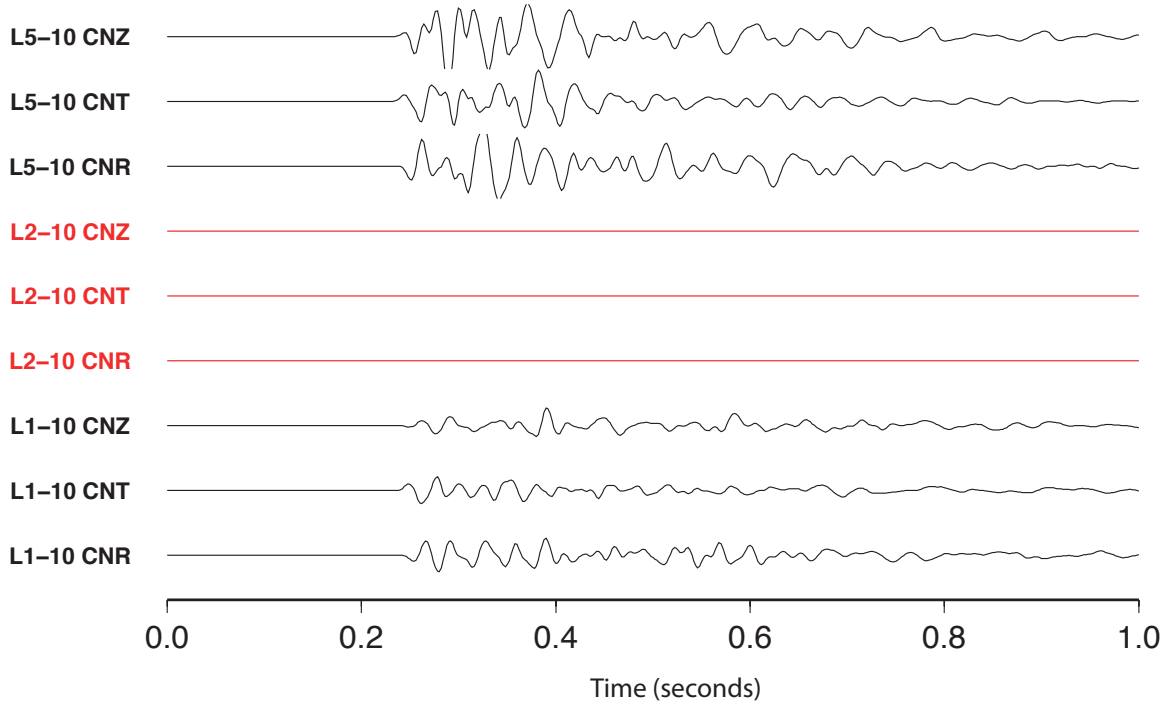


Figure 11. Episensors (acceleration) data. Station L2-10 appears dead.

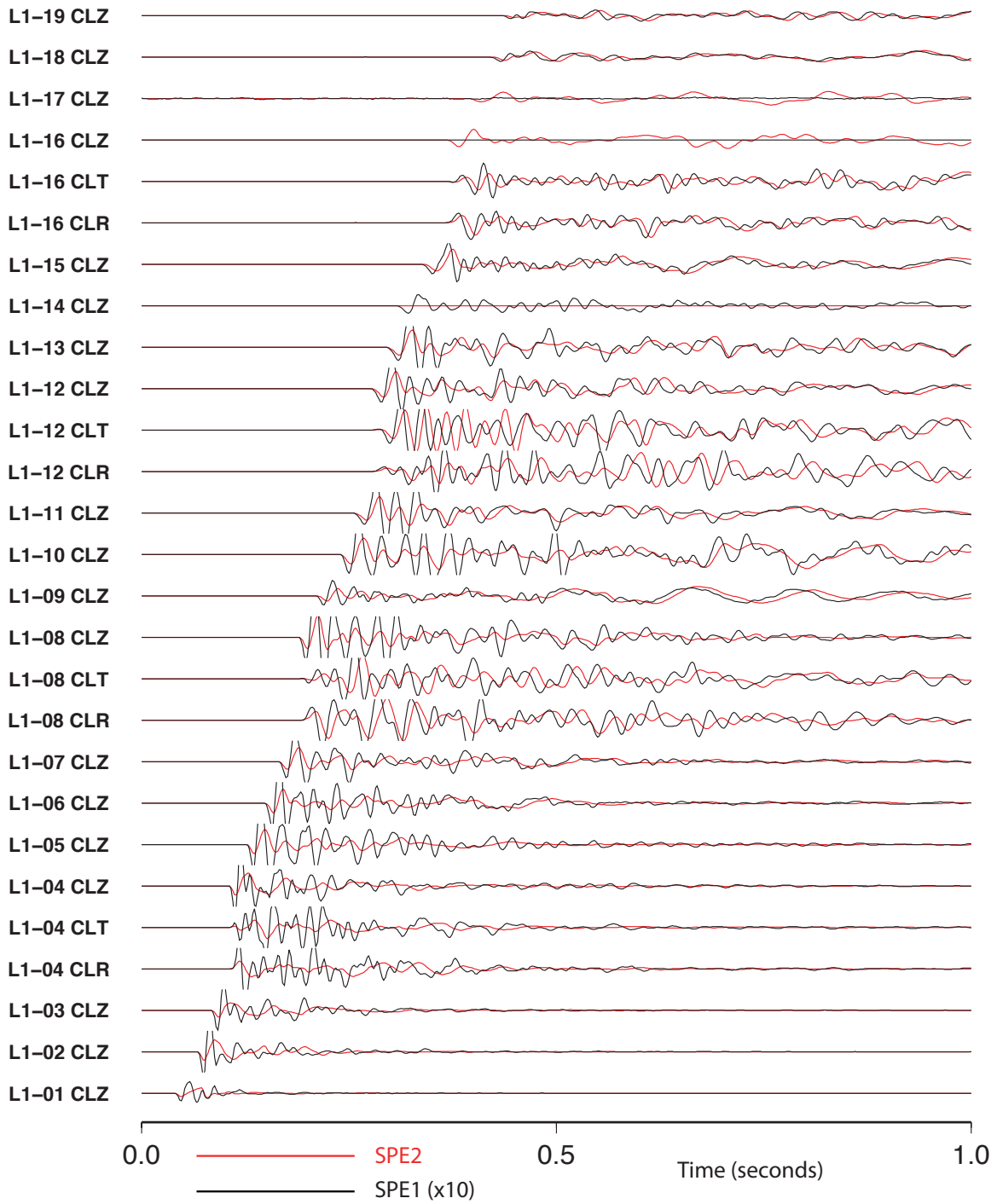


Figure 12. Comparison between SPE1 (x10) and SPE2.

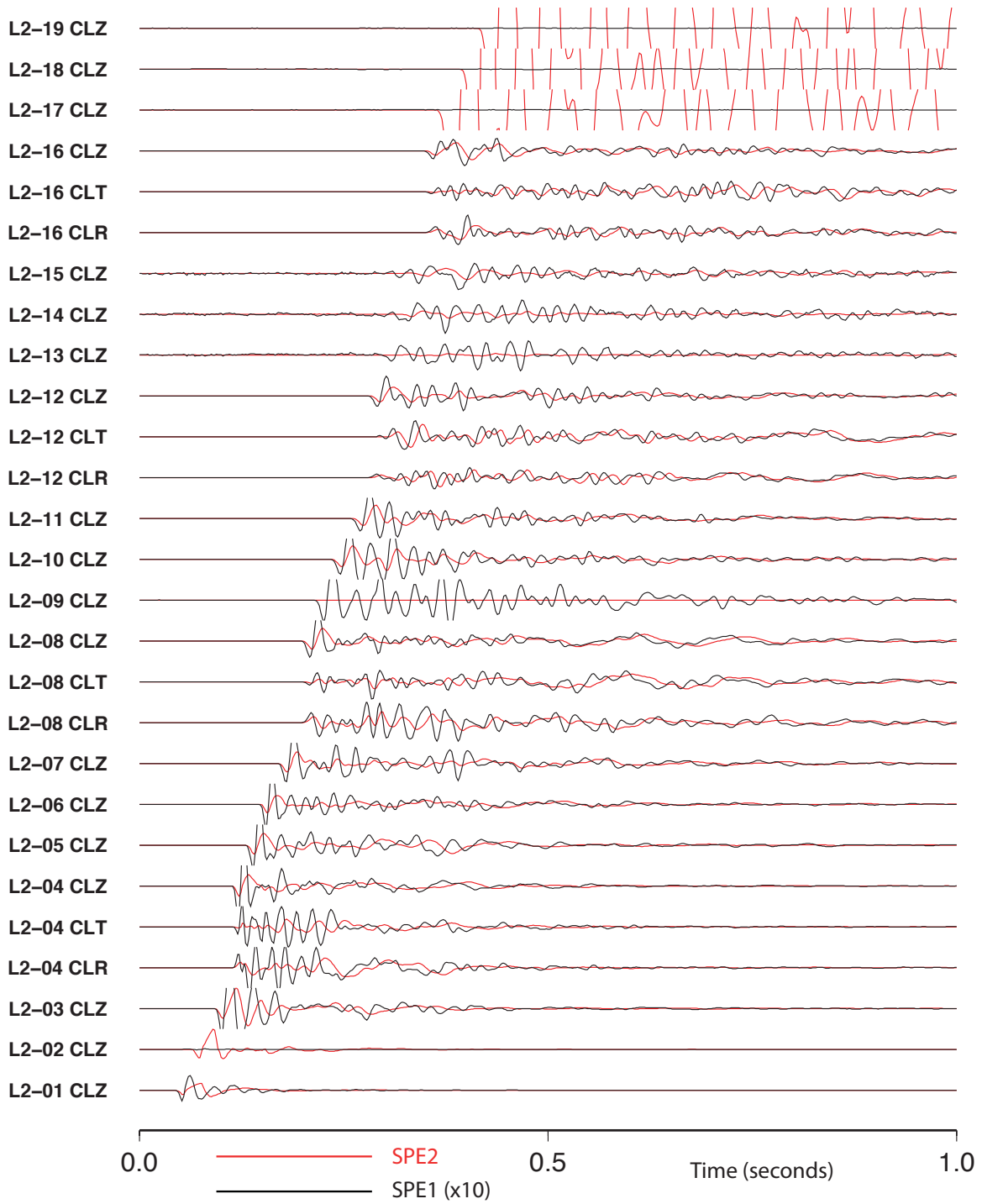


Figure 13. Comparison between SPE1 and SPE2.

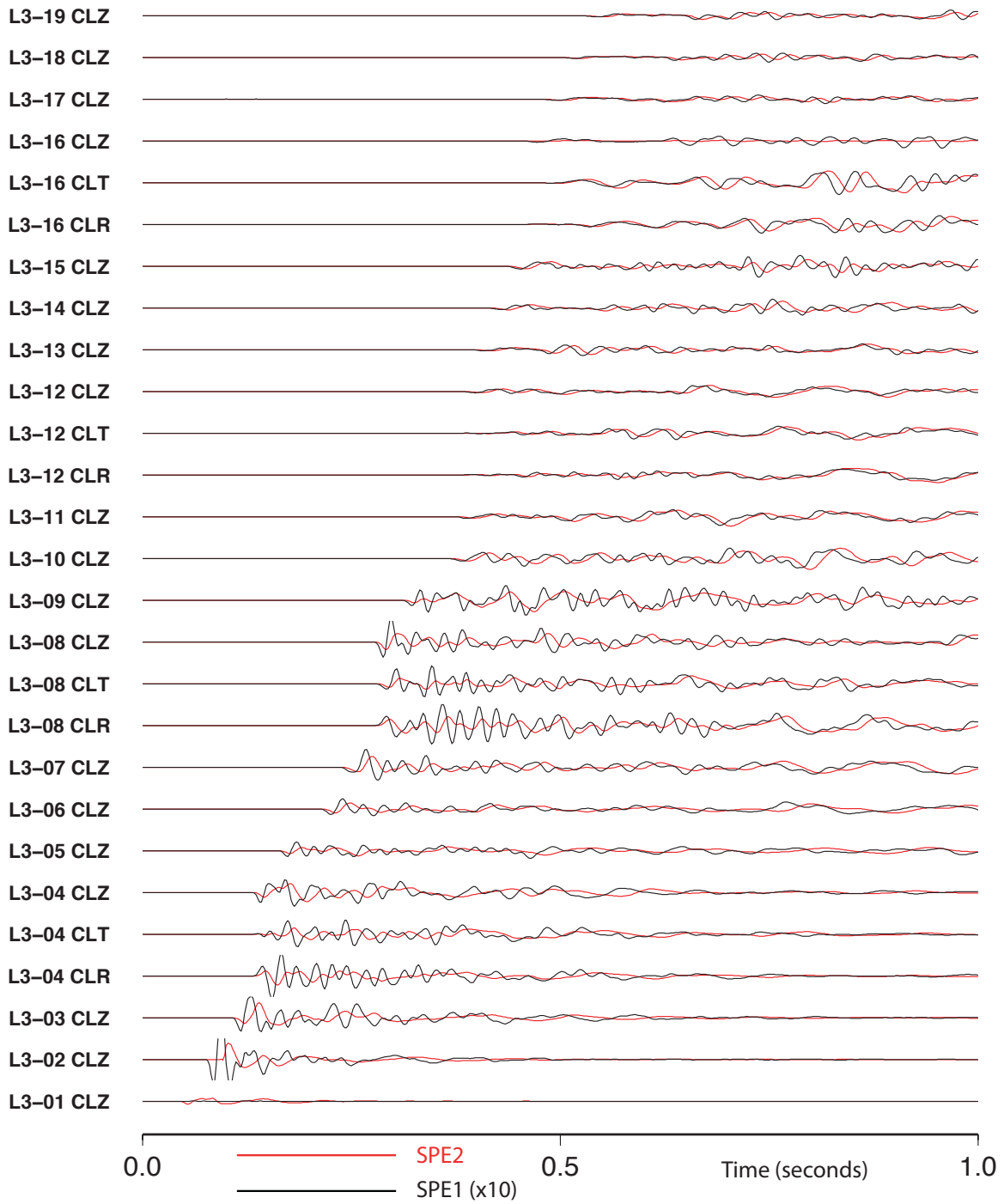


Figure 14. Comparison between SPE1 and SPE2.

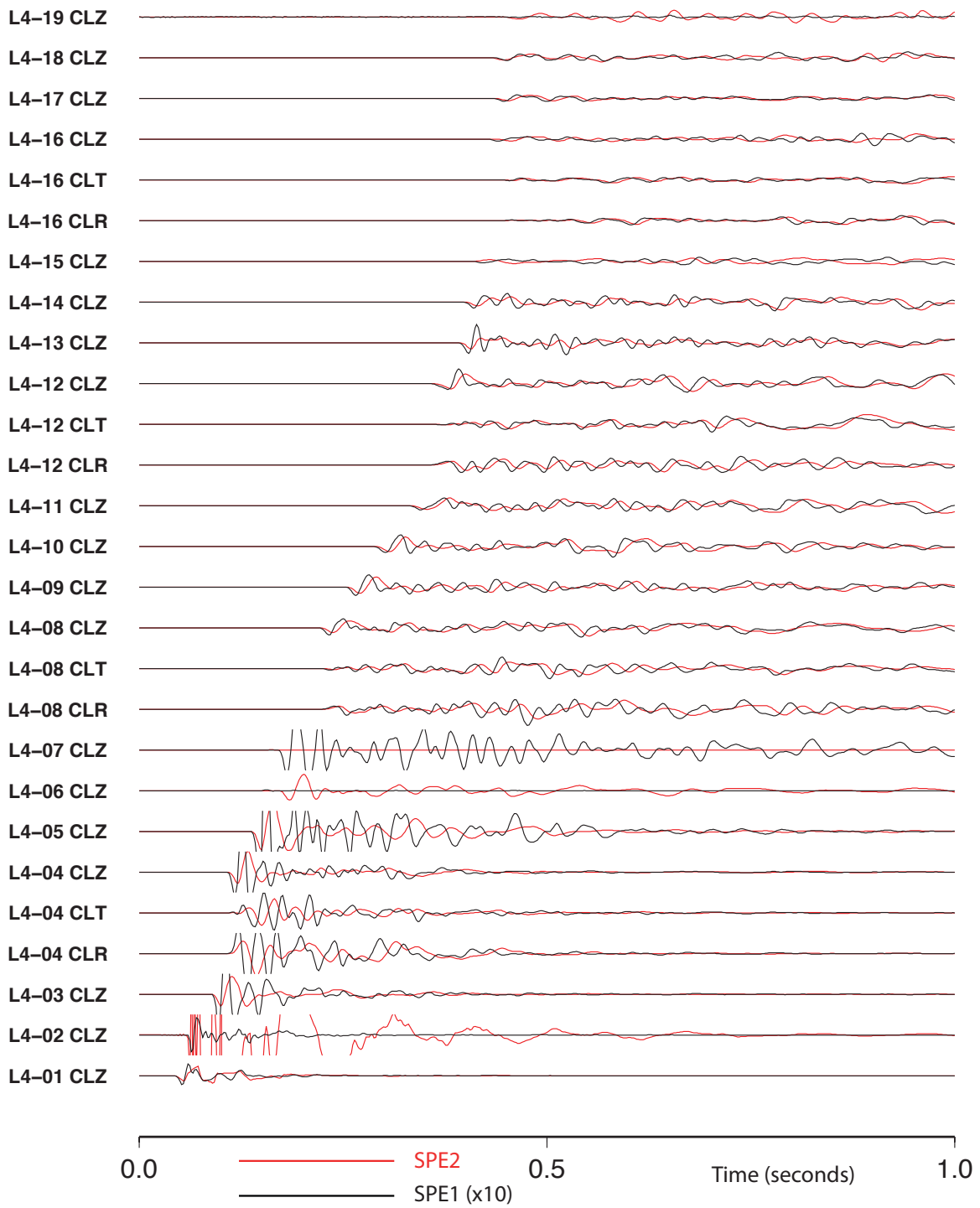


Figure 15. Comparison between SPE1 and SPE2.

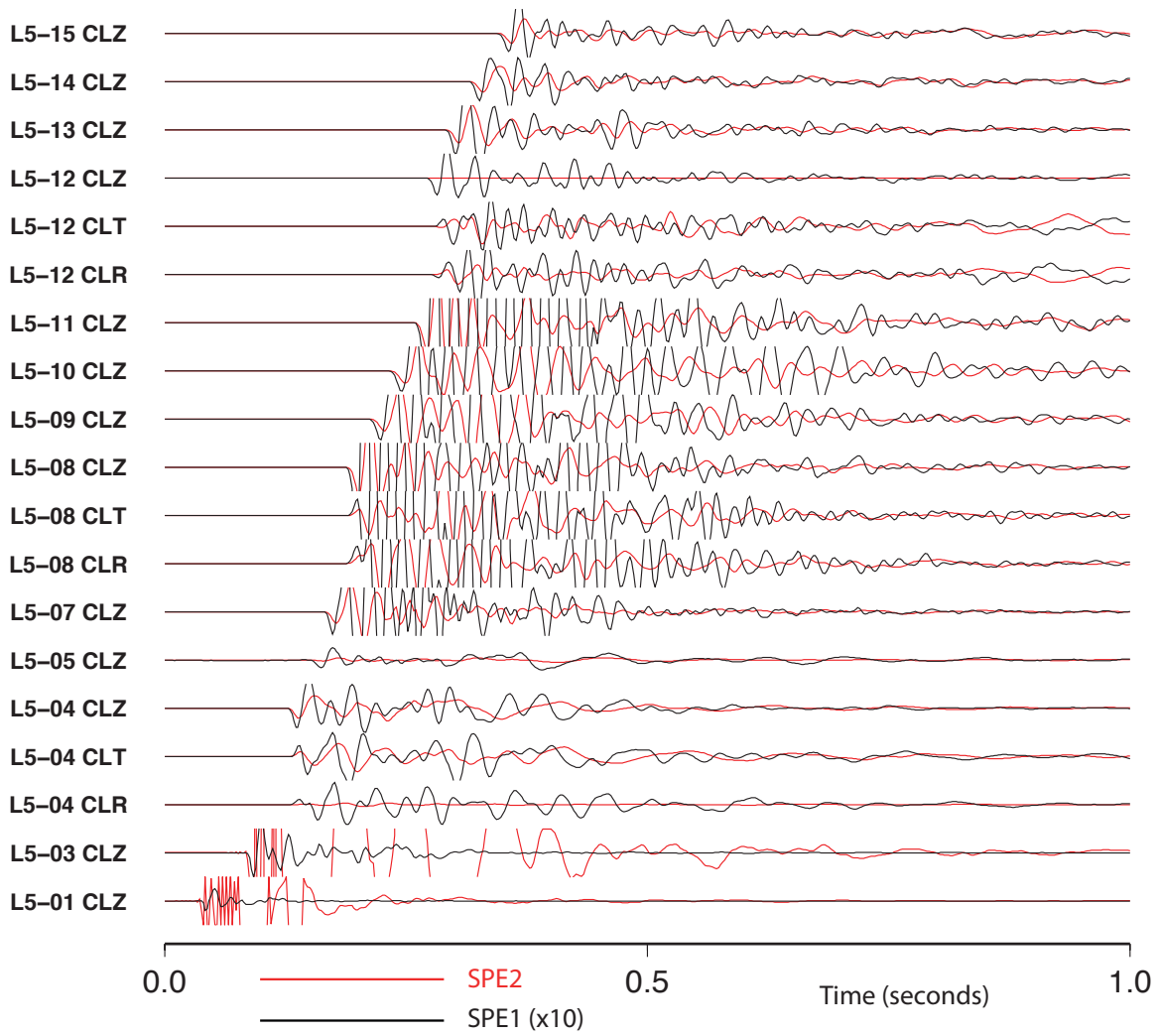


Figure 16. Comparison between SPE1 and SPE2.